Sunlit coponents' fractions and gap fraction of canopies based on POV-ray

WANG Jiangeng[1,2,3], ZHAO Feng[4,2,3], LI Hu[1], YU Tao[2,3], GU Xingfa[2,3], XUE Lian[2,3], YE Lizao[1]

1. *Fujian Provincial Laboratory of Subtropical Resources and Environment, School of Geographical Sciences, Fujian Normal University, Fujian Fuzhou* 350007, *China*;
2. *State Key Laboratory of Remote Sensing Science, Jointly Sponsored by the Institute of Remote Sensing Applications of Chinese Academy of Sciences and Beijing Normal University, Beijing* 100101, *China*;
3. *The Center for National Space borne Demonstration, Beijing* 100101, *China*;
4. *Key Laboratory of Precision Opto-Mechatronics Technology, Ministry of Education, School of Instrument Science and Opto-Electronics Engineering, Beijing University of Aeronautics and Astronautics, Beijing* 100191, *China*

Abstract: The fractions of four components (sunlit leaves, shaded leaves, sunlit soil and shaded soil) and gap fraction are characteristic geometric parameters of canopy's structure, and have great influence on radiative transfer of the vegetation. In this paper, POV-ray software was introduced to efficiently and accurately calculate the four components' fractions and gap fraction of three-dimensional (3D) canopies. With the good agreements of computed four components' fractions and gap fraction between POV-ray and Radiosity-Graphics combined Model (RGM) based on the same 3D canopy structure, more 3D structures generated by the Clumped Architecture Model of Plants (CLAMP) model were used to study the characteristics of four components' fractions and gap fraction. The key parameters of CLAMP model include sowing scheme, clumping index, average leaf angle (ALA) and leaf area index (LAI). By analyzing the sensitivity of these parameters to four components' fractions and gap fraction, the changing features of four components' fractions and gap fraction were found. The results show that: clumping index can effectively control the spatial distribution of leaves, which affects the relative proportion of vegetation and soil in the scene. Therefore, clumping index has a great impact on the distribution pattern of four components' fractions and gap fraction. Average leaf angle influences the anisotropy of the results. When the average leaf angle is larger, the magnitude of anisotropy is higher. Compared with other parameters, the impact of row effect on the four components' fractions and gap fraction is primary when the scene's row structure is obvious. Therefore, when the canopy is in a row structure, the characteristic change of four components' fractions and gap fraction is more complex than that of homogeneous canopy. At the same time, the results of row canopy in three typical growing stages were compared, which shows that soil has a higher contribution to the four components' fractions and gap fraction than that of vegetation at the early stage. With the increase of leaf area index, the influence of vegetation on the result is gradually enhanced and the fraction of sunlit leaves shows more apparent anisotropy. The research of this paper shows that POV-ray is a powerful tool to quantitatively study vegetation by remote sensing technology, and has potential of wider applications.

Key words: POV-ray, CLAMP model, four components' fractions, gap fraction

CLC number: TP751.1/TP79 **Document code:** A

Citation format: Wang J G, Zhao F, Li H, Yu T, Gu X F, Xue L and Ye L Z. 2010. Sunlit coponents' fractions and gap fraction of canopies based on POV-ray. *Journal of Remote Sensing*. **14**(2): 232—251

1 INTRODUCTION

The fractions of four components (sunlit leaves, shaded leaves, sunlit soil and shaded soil) and gap fraction are characteristic geometric parameters of canopy's structure, which are important to affect radiation transfer of the vegetation. Jackson *et al.* (1979) developed a model that based on the four components' fractions for calculating the directional reflectance of the row structure canopy where the row crops were abstracted as rectangular solids. In the simulation of maize directional brightness temperature, Kimes (1983) developed a model that took into account the canopy architecture in computing the radiative transfer within the vegetation. To describe canopy geometric and thermal characteristics, plant rows were abstracted as extended opaque hedgerows. The canopy was assumed to have four brightness temperature components: the

Received: 2008-07-25; **Accepted**: 2009-03-06

Foundation: National Found for Fostering Talents of Basic Sciences (No. J0830521), Chinese Natural Science Foundation (No. 40901156), Knowledge Innovation Program of the Chinese Academy of Sciences(No. kzcx2-yw-303), Chinese Defence Advance Research Program of Science and Technology , China (No. 2006A01A0200 and No. 07K00100KJ), and State Key Laboratory of Remote Sensing Science (No. 2009kfjj022).

First author biography: Wang Jiangeng (1982—), male. He achieved his BS degree in Nanjing University of Information Science & Technology. He is now pursuing a MSc degree in Fujian Normal University, focusing on quantitative remote sensing. E-mail: wjg0932@yahoo.com.cn

Corresponding author: Li Hu, E-mail: lihu2881@yahoo.com.cn

sunlit and shaded leaves, the sunlit and shaded soil. Each component had a unique brightness temperature. However, the effect of gaps within the plant rows was neglected. According to the actual situation in sparse forest, Li and Straher (1985, 1986) proposed a geometric-optics model by building a relationship between the spare forest's main parameters (plant density, canopy size and height, *etc.*) and four scene components to calculate directional reflectance of forest.

Gap fraction is one of the key variables governing radiative transfer processes in vegetation canopies, with applications to light interception and reflectance simulations. Gap fraction is defined as the probability of a light beam to pass through the canopy without any collision. It is determined by the canopy architecture (Gower *et al.,* 1999). Four components' fractions and gap fraction are dimensionless quantities between 0 and 1.

The methods of studying four components' fraction and gap fraction could be classified into three types, which include: (1) experimental methods; (2) analytical models; and (3) computer/numerical simulation methods. Experimental methods are time-consuming and laborious, and have many uncontrollable sources of error (Bruno *et al.*, 1994); analytical models, in order to solve the radiative transfer equation, adopt some assumptions that simplify the geometric structure of the canopy. However, actual vegetation canopies have complex three-dimensional structure characteristics, so the applications of such models have limitations to meet their assumption (Kimes *et al.*, 1985); computer/numerical simulation methods can serve to generate various types of flexibility in the canopy, and to simulate the vegetation structural characteristics in different growth stages from simple to complex structures. With the fast development of computer technology, more and more scholars focus on these methods (Goel *et al.*, 1991).

In this paper, POV-ray (Persistence of Vision Ray-tracer, POV team, 2004) was introduced to efficiently and accurately calculate the four components' fractions and gap fraction of 3D canopies generated by the Clumped Architecture Model of Plants (Nadia *et al*., 2002). By varying the key structural parameters of CLAMP, the changing features of four scene components and gap fraction in different geometric structure were studied.

2 METHOD AND VALIDATION

In this section, firstly POV-ray was introduced. Then its systematic parameters were explained by the sensitivity analysis. Based on the analysis, appropriate systematic parameters were chosen to calculate the four components' fractions and gap fraction by POV-ray afterwards. The good agreements of the computed four components' fraction and gap fraction between POV-ray and Radiosity-Graphics combined Model (RGM, Qin & Gerstl, 2000) base on the same canopies, demonstrated the reliability of applying the POV-ray to compute the four components' fractions and gap fraction. The canopy scenes here used to evaluate the POV-ray are row structure and homogeneous canopies. Leaves are represented by triangles with an erectophile distribution, randomly distributed in the canopy scenes. Canopy structural parameters are listed in Table 1.

2.1 POV-ray

POV-ray (version 3.6, POV team, 2004) is a ray-tracing software devoted to image synthesis, which adopts reverse ray tracing method. POV-ray can simulate the interactions between rays and objects (plants, leaves *etc*.). In this respect the approach used here is basically different from the one used in Monte Carlo ray-tracing models, where stochastic sampling thchniques are used to simulate the interactions between rays and objects, based on probability density functions describing objects scattering behavior (Govaerts & Verstraete, 1998). The output of POV-ray is an image, which is helpful to understand and analysis the results. The POV-ray scripting language for the scene description is very flexible and portable between different computer platforms (POV team, 2004).

Table 1 Canopy statistical structure parameters used by sensitivity analyses of POV-ray's systematic parameters and comparison with RGM

	LAI	Plant height /cm	Row distance /cm	Row width /cm	ALA /(°)	max area of leaves /cm^2	min area of leaves /cm^2	average area of leaf /cm^2
Row structure canopy	1.28	30	50	20	61.89	12.5	0.2	10.7
homogeneous canopy	4.89	100	-	-	63.57	12.5	0.3	10.9

As a kind of efficient, simple and user-friendly software, POV-ray has been widely used in biochemistry, circuit simulation, architectural design and 3D landscape generation and so on. Moreover, due to its characteristics of open source, the algorithms will be continuously improved and optimized. In recent years, a few scholars tried to introduce POV-ray to the remote sensing community. Using this approach it has been possible to simulate the light environment in canopies (Sinoquet *et al*., 1998) and inverse LAI from multiangular images (Casa & Jones, 2005).

2.2 POV-ray systematic parameters sensitivity analysis

The POV-ray outputs 24-bit color images. According to the definition of four components' fractions and gap fraction, their results were obtained by calculating the ratio of different fractions' pixels numbers to those of the image. By analyzing the imaging process, three systematic parameters can influence the final results of POV-ray, namely: field of view (FOV), the camera distance away from the ground and the image resolution. The canopy scene used to study the sensitivity of the systematic parameters is the row structure canopy in Table 1. The row direction is north-south oriented. The number of triangular leaves is 76800. The sun azimuth angle (SAA) is 140° (the north direction is assumed to be the origin with an azimuth angle of 0°. The azimuths of the south, the east, and the west are 180°, 90°, and 270°, respectively). The solar zenith angle (SZA) is 40°. The results of the principal plane (the view azimuth angle (VAA) is 140° or 320°) were shown for sensitivity analysis. The view zenith angle (VZA) changes from forward 60° (VAA equals 320°) to backward 60° (VAA equals 140°) with an interval of 5°. Fig. 1 shows the sample result of POV-ray with VAA and VZA equaling 140° and –45° respectively, in which the green parts represent the sunlit leaves, the black parts represent the shaded leaves, the white parts represent the sunlit soils and the gray parts represent the shaded soils, respectively. The sunlit fractions play a more important role for the radiative transfer than the shaded fractions, so just the sunlit fractions' results were shown in the later analysis.

2.2.1 FOV

The FOV is the key parameter of camera, which determines the visible field size. It could be expressed as:

$$S = (2 \times H \times \tan(FOV/2))^2 \quad (1)$$

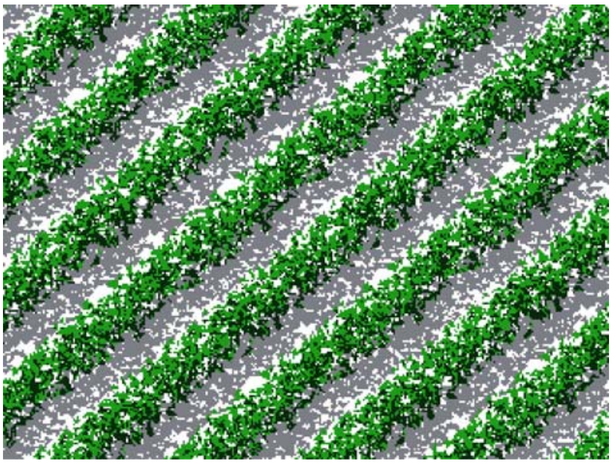

Fig. 1 Image rendered by POV-ray

where *S*, the visible area, depends on FOV and the camera's distance away from the ground (*H*) by Eq. (1). Here FOVs of 0.01°, 0.5°, 10°, 20° and 30° were selected for sensitivity analysis. To ensure the visible area does not exceed the boundary of the scenes at different angles, it was set as 9.329m^2. To keep *S* constant with changing of FOV, *H* correspondingly changed, with 17500, 350, 17.46, 8.66 and 5.7m, respectively. Output image resolution is the systematic default of 320×240. Then the size of each image pixel is 1.215m^2. Fig. 2 shows the distributions of sunlit leaves fraction, sunlight soil fraction and gap fraction in the principal plane with different FOVs. No significant differences were found in sunlit leaves and soils' fractions (as shown in Fig.2 (a) and Fig. 2(b)) for FOVs ranging from 0.01° to 30° except for a marked decrease in the hotspot peak observed with wider FOVs; Fig.2 (c) shows the gap fraction at the vicinity of zenith have some differences: the larger the FOV, the smaller the value of gap fraction. There are very small differences between 0.05° and 0.1°. Because the smaller FOV needs much more computation time, we fixed the FOV as 0.5° for later calculations.

2.2.2 Camera distance

According to Eq. (1), under the same FOV, the camera's distance from the ground (*H*) determines the visible area (*S*) and the number of leaves in the view, thereby affecting the results of the four components' fractions and gap fraction. Here different values of 50, 200, 350 and 500m for *H* were chosen to carry out the sensitivity analysis. Correspondingly, *S* equals 0.19, 3.046, 9.329 and 19.039m^2. The FOV was fixed to 0.5° as mentioned above and the output image resolution is 320×240. The image pixel, equals 0.025, 0.397, 1.215 and 2.479cm^2, respectively. Fig. 3 shows the distributions of sunlit leaves fraction, sunlight soil fraction and gap fraction in the principal plane with the different camera's distance from the ground. When *H* equals 50m, the visible area is 0.19m^2. Because the unit area of the row canopy is 0.25 m^2, and the visible area can't include one row unit, the results show fluctuations. When the visible area is lager than one row unit, the results of four scene components and gap fraction are stable. Taking into account the computing efficiency and visual analysis, a smaller camera distance was chosen with the condition of inclusion of

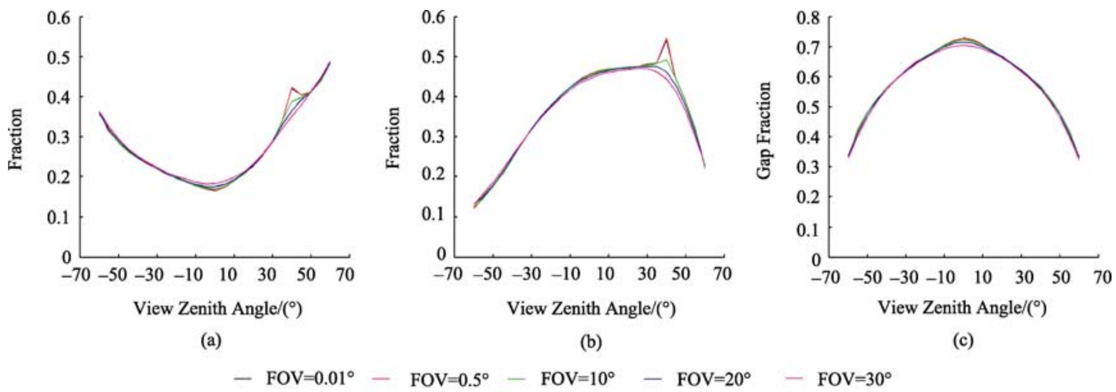

Fig. 2 Distributions of sunlit leaves fraction(a), sunlight soil fraction (b) and gap fraction (c) in the principal plane with different FOVs

at least one whole unit of row canopy.

2.2.3 Image resolution

Image resolution is a measurement of the distinguishability in an image. Here four kinds of image resolution for sensitivity analysis, namely, 160×120, 320×240, 640×480 and 1280×1024 were chosen. By setting FOV as 0.5° and *H* as 50m, the visible area is 9.329 m^2. With the above four resolutions, corresponding image pixel sizes are 4.859, 1.215, 0.304 and 0.071 cm^2, respectively. The time required to output the images, are 247, 289, 340 and 575s, respectively. Fig. 4 shows the distributions of sunlit leaves fraction, sunlight soil fraction and gap fraction in the principal plane with different image resolutions. The results don't show any discernable differences, because the average leaf size is 10.7cm^2, larger than the pixel sizes of above four image resolutions. Taking into account the computing time and visual analysis, we set a low image resolution in the later calculations.

2.3 Validating the results of POV-ray

RGM was developed by Qin & Gerstl (2000) based on the radiosity method (Goel *et al.*, 1991). Comparison results with other 3D radiative transfer models show good agreements (Pinty *et al.*, 2004, Widlowski *et al.*, 2007). Recently some researchers (Wu *et al.*, 2002, Xie *et al.*, 2003, Huang *et al.*, 2006, Song *et al.*, 2007 and Liu *et al.*, 2007) have improved and extended the model.

POV-ray allows the definition of the elements of the scene from numerous shapes, also the geometry (i.e. location and direction) of the light sources illuminating the scene, and that of the camera looking at the scene. The advantage of using POV-ray is that the scripting language for the scene description is effectively and fully functional programming language (POV-team, 2004). By using its scripting language, the four components' fractions and gap fraction can be calculated by POV-ray. RGM is based on the principle of radiosity method to calculate the radiative transfer process between the polygonal elements. Therefore, RGM need not only the geometrical relationships between the light source, camera and objects, but the spectral information, such as the light source characteristics, reflectance and transmission of the objects and so on. RGM can calculate the bi-directional reflectance and albedo etc. (Qin & Gerstl, 2000). Four components' fractions are intermediate results generated in the process of calculation, but as the characteristic parameters of the canopy its do not change along with the input spectral parameters. To evaluate the reliability of the four components' fractions calculated by POV-ray, here we

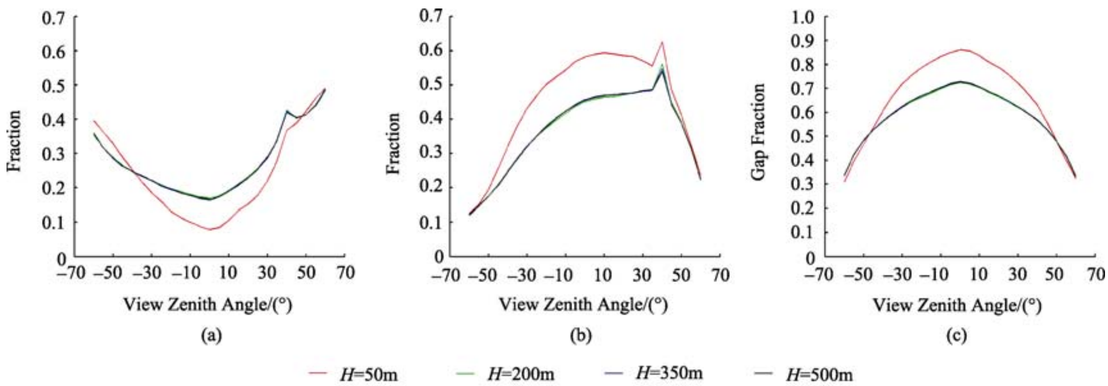

Fig. 3 Distributions of sunlit leaves fraction (a), sunlight soil fraction (b) and gap fraction (c) in the principal plane with the different camera's distance from the ground

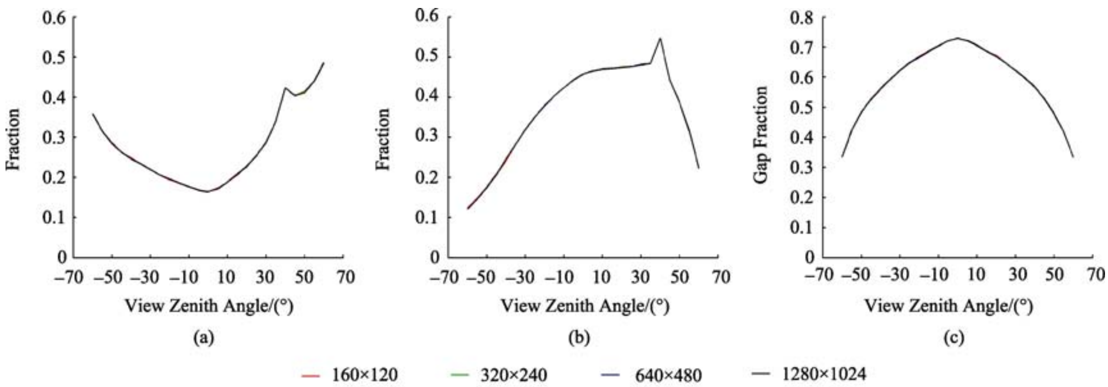

Fig. 4 Distributions of sunlit leaves fraction (a), sunlight soil fraction (b) and gap fraction(c) in the principal plane with different image resolutions

carried out the comparisons between RGM and POV-ray under the same 3D scenes and sun-observer geometries.

The structural parameters of canopies for comparisons were listed in Table 1. Fig. 5 shows the polar contour maps of RGM and POV-ray, with VZA from 0° to 360° at an interval of 10° and VAA from 0° to 60° at an interval of 5° (522 results for comparisons). Table 2 gives the correlation coefficients and RMSEs between these two models. The results show that two models have good agreements.

Through making the sensitivity analysis of the POV-ray's systematic parameters (FOV, the camera distance from the ground and the image resolution), we selected the appropriate systematic parameters of POV-ray to calculate the four components' fractions and compared its results with those of RGM for the same 3D scenes and sun-observer geometries, which proved that the reliability of using POV-ray to calculate the four components' fractions.

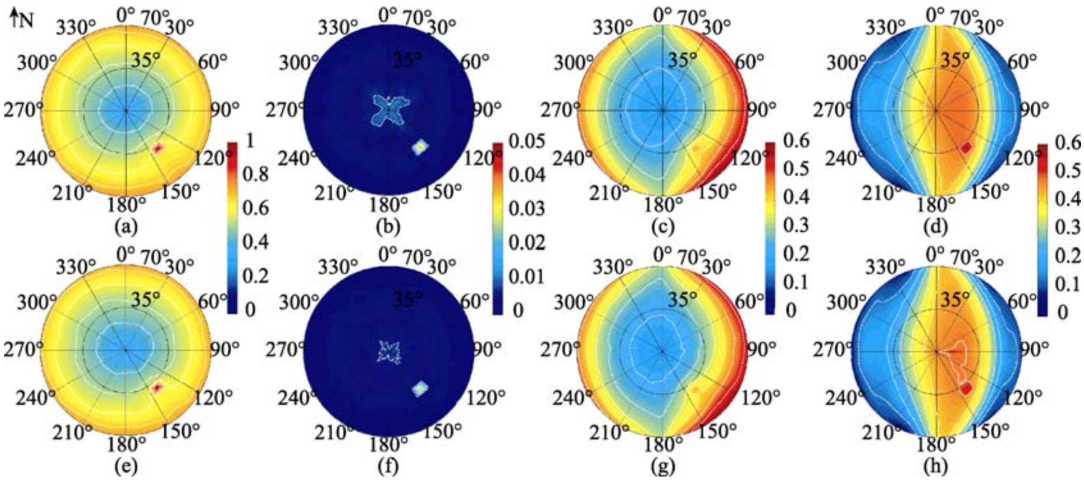

Fig. 5 Polar contour maps of RGM and POV-ray. Homogeneous vegetation: RGM's sunlit leaves fraction (a) and sunlit soil fraction (b), POV-ray's sunlit leaves fraction (e) and sunlit soil fraction (f); Row structure: RGM's sunlit leaves fraction (c) and sunlit soil fraction (d), POV-ray's sunlit leaves fraction (g) and sunlit soil fraction (h)

Table 2 Statistical results of POV-ray and RGM model fitting

Row structure canopy	Sunlit leaves	Shaded leaves	Sunlit soil	Shaded soil	homogeneous canopy	Sunlit leaves	Shaded leaves	Sunlit soil	Shaded soil
R^2	0.9993	0.9990	0.9988	0.9995	R^2	0.9976	0.9930	0.9491	0.9991
RMSE	0.0038	0.0030	0.0079	0.0082	RMSE	0.0137	0.0125	0.0016	0.0033

3 APPLICATION

3.1 CLAMP model

With the minimum possible input parameters, CLAMP model can generate three dimensional canopy scenes efficiently, which explicitly describes the non-random distribution of canopies at the stand and leaf level. A detailed description of this model was given in Rochdi *et al*. (2002).The input parameters of CLAMP model are: sowing scheme (*R*), plant density (d), clumping index (*X*), leaf relative size (*S*, hot spot parameter, Kuusk, 1985), the average leaf angle (ALA, Campbell, 1990), leaf shape parameter (*B*, the ratio of isosceles triangle leaf between the bottom and the height) and leaf area index (LAI).

3.2 Sensitivity analysis of CLAMP parameters

In this section, key parameters of CLAMP were used to study the changing characteristics of four components' fractions and gap fraction computed by POV-ray. Settings of POV-ray systematic parameters are as follows: FOV=0.5°, the camera distance from ground (*H*) = 60m and the image resolution is 320×240. So the field size (*S*) equals 0.273m^2 and the corresponding pixel size equals 0.036cm^2. The leaf area equals 0.115 cm^2.

3.2.1 *The sensitivity analysis of sowing scheme and clumping index*

The radiative transfer of the row crops and homogeneous canopies have significant difference (Jackson, 1979; Zhao *et al.*, 2009). CLAMP controls the spatial distribution of plants by changing sowing scheme (*R*): With *R* equaling 1, leaves randomly distribute in the cuboids limited by the row distance, row width and row height; With *R* equaling 0, leaves continuously distribute in the canopy scene. The horizontal distance between leaves and the corresponding stem is described by the clumping index (*X*): with *X* equaling 0, the horizontal distance between leaves and the corresponding stem is 0, namely leaves attach the stem; with *X* equaling 1, leaves randomly distribute in the canopy (no clumping effect). When clumping index varies from 0 to 1, leaves are correspondingly change in the degree of concentration.

In this paper, sensitivity analysis was performed to four extreme instances, R_0X_0 (homogeneous canopy with leaves attaching the stem closely); R_0X_1 (homogeneous canopy with randomly distributed leaves); R_1X_0 (row structured canopy with leaves attaching the stem closely); R_1X_1 (row structured canopy with randomly distributed leaves). The row direction is oriented in the north-south direction. Input parameters for CLAMP model are listed in Table 3.

In Fig.6, the fractions of sunlit leaves and soil reach their maximums in the sun direction (hot spot). In other azimuthal angles, the sunlit leaves' fractions of two cases in which leaves randomly distribute (X = 1) are greater than the corresponding cases where leaves completely attach the stems, which is due to higher mutual shading probability of leaves for clumping leaves than that for randomly distributed leaves. So, with the increase of VZA, more leaves are directly sunlit and visible for randomly distributed canopies. When the canopies are in row structure (R = 1, as shown in Fig.6(c), Fig.6(d), Fig.6(g) and Fig.6(h)), there are high-value and low-value strips approximately parallel to the row direction in the polar maps, which is the features for typical row canopies, namely the row effect (Zhao *et al.*, 2009). This feature is absent for homogeneous canopies (R = 0, as shown in Fig.6(a), Fig.6(b), Fig.6(e) and Fig.6(f)). When the leaves completely attach the stems (X=0), there are large interspaces between the plants. So sunlit soil fractions are larger than their counter-parts, for example, Fig.6(e)–Fig.6(f), and Fig.6(g)–Fig.6(h), especially for low VZAs.

In Fig.7 (a) and Fig.7 (b), the maximum values of the fractions for sunlit leaves and soil are shown as a peak at the sun position in the profile along the solar principal plane. The sunlit leaves' fractions for the canopies of randomly distributed leaves (X=1) are higher than those of the canopies with clumped leaves (X=0). For the clumped canopies, when the VZAs are low (lower than 20°), the sunlit leaves' fractions of homogeneous canopies (R=0) are higher than those of row structured canopies (R=1). For high VZAs (higher than 20°), the relationship of the sunlit leaves' fractions of these two canopies reverses. The reason for this phenomenon is that the density of leaves in the row is higher than that of homogeneous canopies. Therefore, for high VZAs, more parts of the leaves of the row structured canopies are sunlit and visible. Fig. 7 (c) shows that

Table 3 Input parameters for CLAMP model when *R* and *X* change

R	X	ALA / (°)	LAI	S	B	d / (plants/ m^2)	Row distance / cm	Row width/ cm	Plant height / cm
0; 0; 1; 1	0; 1; 0; 1	58	2	0.2	0.3	400	10	5	20

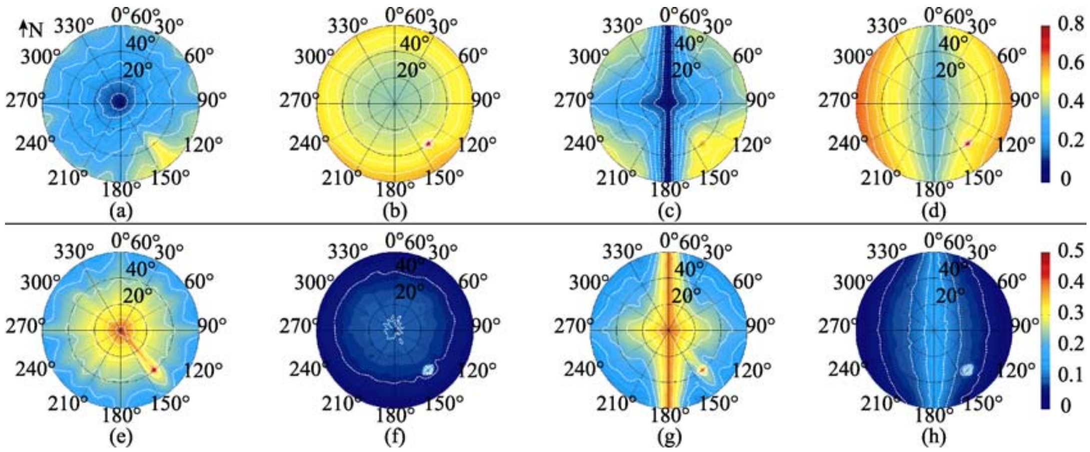

Fig. 6 Polar contour maps with four canopy types. R_0X_0: sunlit leaves fraction (a) and sunlit soil fraction (e), R_0X_1: sulit leaves fraction (b) and sunlit soil fraction (f), R_1X_0: sulit leaves fraction (c) and sunlit soil fraction (g), R_1X_1: sulit leaves fraction (d) and sunlit soil fraction (h)

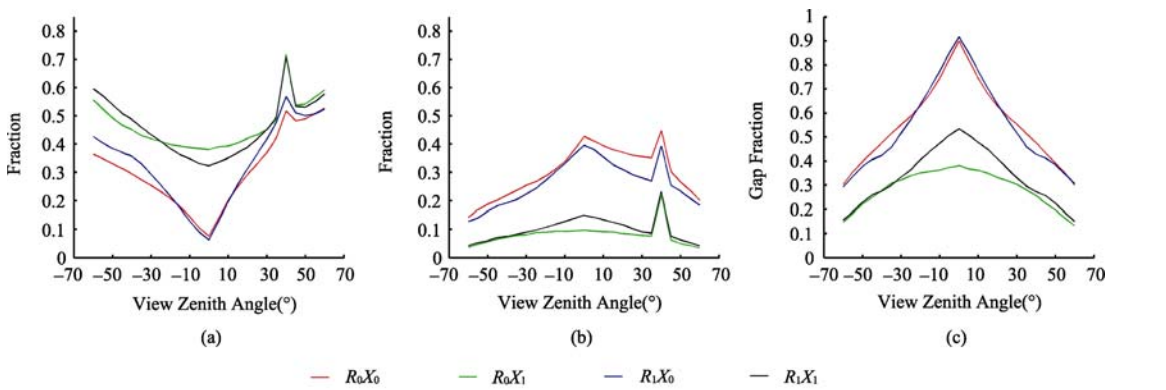

Fig. 7 Fractions' distributions for four canopy types. The principal plane's fractions of sunlit leaves (a), sunlight soil (b) and gap fraction(c)

the clumped canopy has the highest degree of anisotropy, and the anisotropies of row structured canopies (R=1) are more obvious than those of homogeneous canopy (R=0).

3.2.2 Sensitivity analysis of average leaf angle

Leaf angle distribution (LAD) is a key parameter to characterize canopy structure and plays a crucial role in controlling energy and mass balance in soil-vegetation-atmosphere-transfer system. Generally it is assumed that plant leaves have azimuthal symmetry, so that LAD effectively only deals with leaf inclination distribution. CLAMP model adopts the single-parameter (average leaf angle, ALA) ellipsoidal distribution function (Campbell, 1990) to control the leaf angle. Wang *et al.* (2007) compared several widely-used LAD functions, whose results show that the single-parameter ellipsoidal distributions function can faithfully represent the distribution of leaf inclination angle.

In this part, three typical leaf angle distributions were compared: planophile (ALA=10°), spherical (ALA=58°) and erectophile (ALA=75°). Other input parameters for CLAMP model are listed in Table 4.

Fig.8 shows that, with the increase of ALA, row effect and anisotropies of sunlit fractions distributions become more pronounced. In Fig.9 (a) and Fig.9 (b), the maximum value of the fractions of sunlit leaves and soil are shown as a peak at the sun position (SZA=40°, SAA=140°) in the profile along the solar principal plane. When VZA is low, the sunlit leaves' fraction of planophile distribution is the biggest among three patterns. When VZA becomes higher, the sunlit leaves' fraction of erectophile distribution turns up to be the biggest. Similar trends also occur to the distribution of gap fractions (Fig.9 (c)).

Table 4 Input parameters for CLAMP model when ALA changes

ALA / (°)	LAI	R	S	X	B	d / (plants/m^2)	Row distance / cm	Row width / cm	Plant height / cm
10; 58; 75	2	1	0.2	1	0.3	400	10	5	20

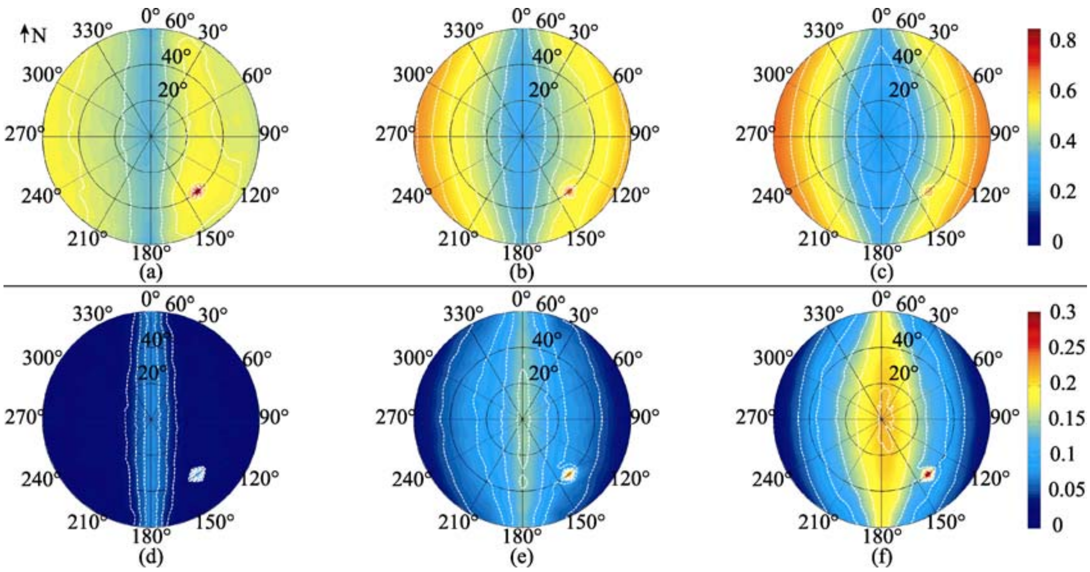

Fig. 8 Polar contour maps with three LAD distributions. ALA=10°: sunlit leaves fraction (a) and sunlit soil fraction (d); ALA=58°: sunlit leaves fraction (b) and sunlit soil fraction (e); ALA=75°: sunlit leaves fraction (c) and sunlit soil fraction (f)

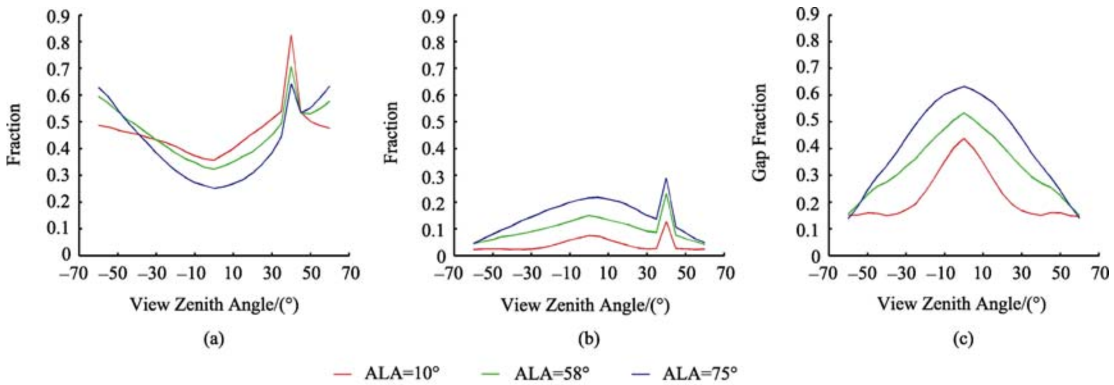

Fig. 9 Fractional distributions with three ALA types. The principal plane's sunlit leaves fraction (a), sunlight soil fraction (b) and gap fraction(c)

3.2.3 Sensitivity analysis of leaf area index

Leaf area index is another key parameter to characterize canopy structure, which is defined as the total one-sided area of leaves above unit area of soil. LAI depends on species composition, developmental stage, prevailing site conditions, seasonality, and the management practices, which controls the vegetation in many physiological and physical processes, such as photosynthesis, respiration and transpiration *etc*. (Jonckheere *at al.*, 2004).

In this part, three LAI values (1, 2 and 4) at typical row crops' growth stages were chosen to perform the sensitivity analysis. The row distance kept constant, but the row width and clumping index were changed proportionally along with the change of LAI. Input parameters for CLAMP model are listed in Table 5.

When LAI (LAI=1) is small and leaves clump in the canopy, there are large gaps among leaves. So the fraction of sunlit soil (Fig. 10(a)) is the largest and that of sunlit leaves (Fig. 10(d)) is minimum among these three canopies. What's more, row effect and hot spot is relatively weak. With the enlargement of row canopy's biomass, these latter two features become evident.

In Fig.11 (a), for the case of LAI = 1, the hot spot of sunlit leaves' fraction is not obvious and the values are smaller than the other two cases. Meanwhile, the sunlit soils and gap fraction have the biggest values. For the medial case (LAI = 2), the hot spot effect and anisotropy are the most prominent in three cases.

Table 5 Input parameters for CLAMP model when LAI changes

	LAI	*X*	Row width / cm	ALA / (°)	*R*	*S*	*B*	*d* / (plants/ m^2)	Row distance / (cm)	Row height / (cm)
Early stage	1	0.3	3	58	1	0.2	0.3	400	10	20
Middle stage	2	0.5	5	58	1	0.2	0.3	400	10	20
Late stage	4	0.8	9	58	1	0.2	0.3	400	10	20

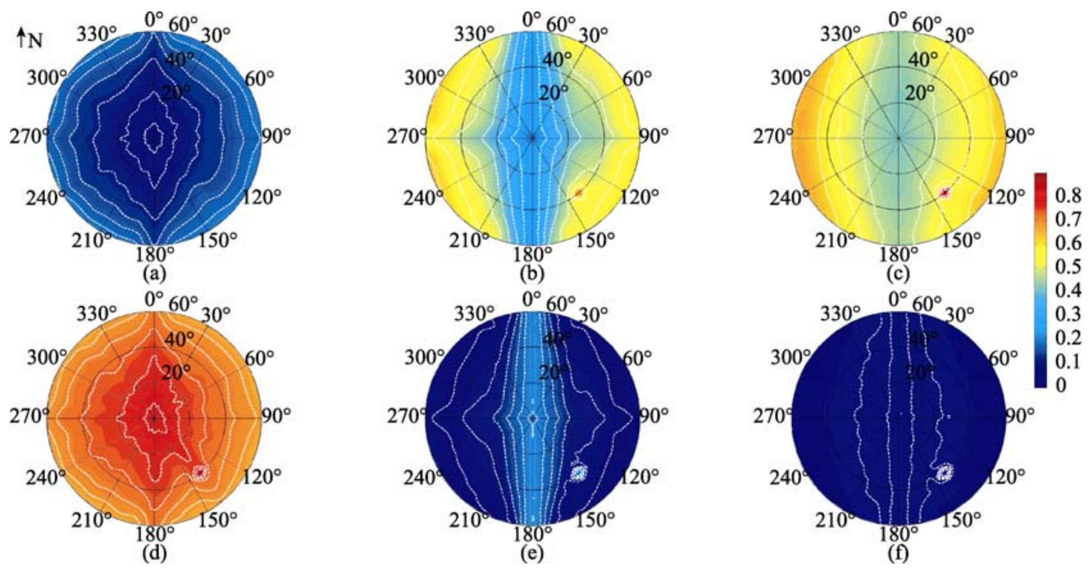

Fig. 10 Polar contour maps with three LAI values. LAI=1: sunlit leaves fraction (a) and sunlit soil fraction (d); LAI=2: sunlit leaves fraction (b) and sunlit soil fraction (e); LAI=4: sunlit leaves fraction (c) and sunlit soil fraction (f)

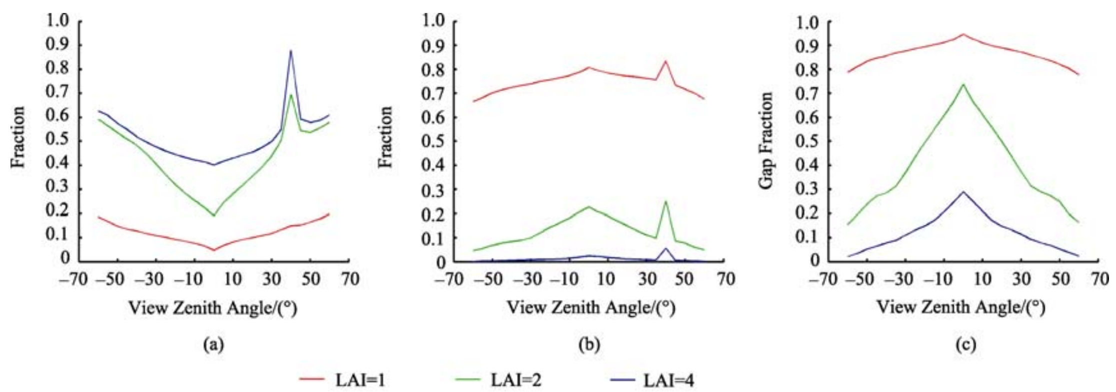

Fig. 11 Fractions' distributions with three LAI values in the principal plane: sunlit leaves fraction (a), sunlight soil fraction (b) and gap fraction (c)

4 CONCLUTION AND DISCUSSION

POV-ray adopts reverse ray-tracing method to render 3D scenes. With its powerful computing ability and simple programming language, POV-ray has been widely applied in 3D scene simulation and visualization. But its application in remote sensing was rarely mentioned. In this paper, POV-ray has been applied to efficiently calculate the four components' fractions and gap fraction of 3D scenes generated by CLAMP model. The results visually display the changing features of four components' fractions and gap fraction. POV-ray is a useful tool for quantitative remote sensing research.

This paper focused on the study of four components' fractions and gap fraction of homogeneous and row structured canopies with different architectures generated by the CLAMP model, such as sowing scheme, clumping index, ALA and LAI. The results show that clumping index can effectively control the spatial distribution of leaves, which affects the relative proportion of vegetation and soil in the scene. Therefore, clumping index has a great impact on the distribution pattern of four components' fractions and gap fraction. ALA influences the anisotropy of the results considerably: the larger ALA is, the higher magnitude of anisotropy is. Compared with other parameters, the impact of row effect on the four components' fractions and gap fraction is primary when the canopy shows clear row structure. Therefore, when the canopy is in a row structure, the characteristic change of four components' fraction and gap fraction is more complex than the homogeneous canopy. The results of row canopy in three typical growing stages were compared, which shows that soil has a higher contribution to the four components' fractions and gap fraction than vegetation at the early stage. With the increase of LAI, the influence of vegetation on the result is gradually enhanced and the sunlit leaves' fraction shows more apparent anisotropy.

This preliminary study shows that POV-ray can be applied to accurately and efficiently calculate the important parameters of vegetation remote sensing (four components' fractions and gap fraction). POV-ray is a powerful tool to study remote sensing of vegetation, and has potential of wider applications.

Acknowledgements: The authors appreciate Professor Casa and POV-ray team for providing useful guidance and help to use POV-ray. They thank Dr. Huaguo Huang at the Beijing Forestry University, Min Chen, Dr. Donghui Xie and Dr. Jinling Song at Beijing Normal University for assistance in the process of comparing POV-ray's results with those by RGM model.

REFERENCES

Bruno A, Yassine S and Nicolas I. 1994. A direct method to measure bidirectional gap fraction in vegetation canopies, *Remote Sensing of Environment*, **50**(1): 61—66

Casa R and Jones H G. 2005. LAI retrieval from multiangular image classification and inversion of a ray tracing model. *Remote Sensing of Environment*, **98**(4): 414—428

Campbell G S. 1990. Derivations of an angle density function for canopies with ellipsoidal leaf angle distributions. *Agricultural and Forest Meteorology*, **49**(3): 173—176

Gower S T, Kucharik C J and Norman J M.1999. Direct and indirect estimation of leaf area index, fAPAR, and net primary production of terrestrial ecosystems. *Remote Sensing of Environment*, **70**(1): 29—51

Goel N S, Rozehnal I and Thompson R L. 1991. A computer graphics based model for scattering from objects of arbitrary shapes in the optical region. *Remote Sensing of Environment*, **36**(2): 73—104

Govaerts Y M and Verstraete M M. 1998. Raytran a monte carlo ray-tracing model to compute light scattering in three-dimensional heterogeneous media. *IEEE Transactions on Geoscience and Remote Sensing*, **36**(2): 493—505

Huang H G, Qin W H, Liu Q H, Liu Q and Li X W. 2006. An extended radiosity-graphics model for directional brightness temperature research. *IGARSS*

Jackson R D, Reginato R J, Pinter P J and Idso S B. 1979. Plant canopy information extraction from composite scene reflectance of row crops. *Applied Optics*, **22**(18) :3775—3782

Jonckheere I, Fleck S, Nackaerts K, Muys B, Coppin P, Weiss M and Baret F. 2004. Review of methods for in situ leaf area index determination Part I. Theories, sensors and hemispherical photography. *Agricultural and Forest Meteorology*, **121**(1—2): 19—35

Kimes D S. 1983. Remote sensing of row crop structure and component temperatures using directional radiometric temperatures and inversion technique. *Remote Sensing of Environment*, **13**: 33—55

Kimes D S, Norman J M and Walthall C L. 1985.Modeling the radiant transfers of sparse vegetation canopies. *IEEE Transactions on Geoscience and Remote Sensing*, **23**(5): 659—704

Kuusk A. 1985. The hot spot effect of a uniform vegetative cover. *Soviet Journal Remote Sensing*, **3**(4): 645—658

Li X W and Strahler A H. 1985. Geometiric-optical modeling of a conifer forest canopy. *IEEE Transactions on Geoscience and Remote Sensing*, **23**(5): 705—721

Li X W and Strahler A H. 1986. Geometiric-optical reflectance modeling of a conifer forest canopy. *IEEE Transactions on Geoscience and Remote Sensing*, **24**(66): 906—919

Liu Q H, Huang H G, Qin W H, Fu K H and Li X W. 2007. An extended 3D radiosity-graphics combined model for studying thermal emission directionality of crop canopy. *IEEE Transactions on Geoscience and Remote Sensing*, **45**(9): 2900—2918

POV-team. 2004. Introduction to POV-Ray for POV-Ray Version 3.6.1. http://www.povray.org

Pinty B, Widlowski J L, Taberner M, Gobron N, Verstraete M M, Disney M, Gascon F, Gastellu J P, Jiang L, Kuusk A, Lewis P, Li X, Ni-Meister W, Nilson T, North P, Qin W, Su L, Tang S, Thompson R, Verhoef W, Wang H, Wang J, Yan G and Zang H. 2004. Radiation transfer model intercomparison (RAMI) exercise: Results from the second phase . *Journal of Geophysical Research*, **109**, D06210, doi:10.1029/ 2003JD 004252.

Qin W H and Gerstl S A W. 2000. 3-D scene modeling of semidesert vegetation cover and its radiation regime. *Remote Sensing of Environment*, **74**(1): 145—162

Rochdi N, Baret, F, Combal B and Chelle M. 2002. CLAMP: A model of leaf clumping in canopies. Recent Advances in Quantitative Remote Sensing, 1st International Symposium, Spain, Publications of the University of Valencia

Sinoquet H, Thanisawanyangkura S, Mabrouk H and Kasemsap P. 1998. Characterization of the light environment in canopies using 3D digitising and image processing. *Annals of Botany*, **82**(2): 203—212

Song J L, Wang J D and Liu X Q. 2007. Computer simulations of difering radiation regimes on aspen trees. *Journal of Remote Sensing*, **11**(5): 669—676

Widlowski J L, Taberner M, Pinty B and Bruniquel-Pinel V, Disney M, Fernandes R, Gastellu-Etchegorry J P, Gobron N, Kuusk A, Lavergne T, Leblanc S, Lewis P E, Martin E, Mottus M, North P R J, Qin W, Rpbustelli M, Rochdi N, Ruiloba R, Soler C, Thompson R,Verhoed W, Verstraete M M and Xie D. 2007. The third radiation transfer model intercomparison (RAMI) exercise: Documenting progress in canopy reflectance modeling. *Journal of Geophysical Research,* 112: doi 10.1029/ 2006JD007821

Wu M X, Zhu Q J, Su L H, Wang J D, Xiang Y Q, Tang S H and Wang P X. 2002. The 3-D scene computer simulation of the field crop canopy. Recent Advances in Quantitative Remote Sensing, 1st International Symposium, Spain, Publications of the University of Valencia

Wang W M, Li Z L and Su H B. 2007. Comparison of leaf angle distribution functions: Effects on extinction coefficient and fraction of sunlit foliage. *Agricultural and Forest Meteorology* , **143**(1—2): 106—122

Xie D H, Wu M X, Zhu Q J, Wang J D and Tang S H. 2003. Quantitative remote sensing research on the vegetation 3-D visual simulation based on object oriented technique. *IEEE International Geoscience and Remote Sensing Symposium*. **6**: 3922—3924

Zhao F, Gu X F, Wout Verhoef, Wang Q, Yu T, Liu Q, Huang H G, Qin W H, Chen L F and Zhao H J, 2010, A spectral directional reflectance model of row crops, *Remote Sensing of Environment* , **114**(2): 265—285

POV-ray 应用于冠层可视光照和阴影组分比例变化分析

王剑庚[1,2,3]，赵 峰[4,2,3]，李 虎[1]，余 涛[2,3]，顾行发[2,3]，薛 廉[2,3]，叶李灶[1]

1. 福建师范大学 地理科学学院，福建省亚热带资源与环境重点实验室，福建 福州 350007;
2. 遥感科学国家重点实验室，中国科学院 遥感应用研究所，北京 100101;
3. 国家航天局航天遥感论证中心，北京 100101;
4. 仪器科学与光电工程学院精密机电一体化技术教育部重点实验室，北京航空航天大学，北京 100191

摘 要： 利用 POV-ray 快速计算三维冠层的四分量比例及孔隙率，在与计算机模拟模型对比结果、验证其可靠性的基础上，针对植被真实结构模型的主要参数对冠层四分量比例和孔隙率的敏感性进行分析。敏感性分析结果表明：当冠层为垄行结构时，相对于其他因素，行结构对四分量比例和孔隙率的影响占主导，因此当植被冠层为垄行结构时，四分量比例和孔隙率的变化较连续冠层更加复杂；集聚指数可以有效的控制叶片的空间分布模式，进而影响到视场中植被与土壤的相对面积比例，对于四分量比例和孔隙率结果有较大影响；叶倾角分布类型对四分量比例和孔隙率结果的各向异性特征影响明显；同时，通过对垄行作物3个典型生长期的四分量比例和孔隙率结果分析得出，在作物生长初期土壤对结果影响更大，在作物生长后期植被对结果的影响占主导，亮叶分量比例各向异性特征较为明显。研究表明，POV-ray 是进行植被定量遥感研究的有利工具，具有较好的应用前景。

关键词： POV-ray, CLAMP 模型，四分量比例，孔隙率

中图分类号： TP751.1/TP79 **文献标识码：** A

引用格式： 王剑庚，赵 峰，李 虎，余 涛，顾行发，薛 廉，叶李灶. 2010. POV-ray 应用于冠层可视光照和阴影组分比例变化分析.遥感学报, **14**(2): 232—251
Wang J G, Zhao F, Li H, Yu T, Gu X F, Xue L and Ye L Z. 2010. Sunlit coponents' fractions and gap fraction of canopies based on POV-ray. *Journal of Remote Sensing*. **14**(2): 232—251

1 引 言

传感器观测到的植被冠层光照叶片、阴影叶片、光照土壤和阴影土壤的面积占传感器视场总面积的比例(简称四分量比例)是植被遥感几何光学建模的重要参数。Jackson 等(1979)通过对四分量比例建模计算行播冠层的反射率；Kimes(1983)将玉米冠层简化为截面无限长、不透光、相互平行的矩形立方体，通过对四分量比例建模得到冠层的方向亮温；Li 和 Straher(1985，1986)根据稀疏林实际情况，采用森林结构的主要参数(株密度、冠层大小和高度等)对四分量比例进行建模，建立了稀疏林 BRDF 模型。孔隙率是光线透过冠层未被拦截到达地表的概率，是视场中亮土和暗土分量比例之和，孔隙率在植被冠层能量平衡估计、水胁迫和多角度信息提取等遥感应用中得到广泛应用(Gower，1999)。四分量比例和孔隙率是无量纲量，值在 0—1 之间。

在植被冠层四分量比例和孔隙率的研究中，常用的方法有 3 种：实验、解析模型和计算机模拟模型。实验方法费时费力，且有很多不可控的误差来源(Bruno 等，1994)；解析模型为了便于辐射传输方程的求解，对冠层的几何结构进行简化假设，但是由于实际植被冠层复杂的三维结构特征，这类模型的应用局限于满足其假设的植被结构类型(Kimes 等，

收稿日期：2008-07-25；修订日期：2009-03-06

基金项目：国家基础科学人才培养基金项目(编号：J0830521)；国家自然科学基金项目(编号：40901156)；中国科学院知识创新工程重要方向项目(编号：kzcx2-yw-303)；国防科技工业民用专项科研技术研究项目(编号：2006A01A0200，07K00100KJ)；遥感科学国家重点实验室开放基金项目(编号：2009kfjj022)。

第一作者简介：王剑庚(1982—)，男，福建师范大学地理科学学院硕士研究生，主要从事定量遥感研究。E-mail: wjg0932@yahoo.com.cn。

通讯作者：李虎，E-mail: lihu2881@yahoo.com.cn。

1985)；计算机模拟模型则具有生成各类冠层的灵活性，可以由简至繁的模拟植被的各种形态及生长结构特征，随着计算机技术的不断发展计算机模拟模型越来越受到学者的重视(Goel 等, 1991)。

本文通过 POV-ray 光线追踪软件(Persistence of Vision Ray-tracer)(POV-team，2004)快速计算植被真实结构模型 CLAMP (the Clumped Architecture Model of Plants)(Nadia 等，2002)生成的三维冠层的四分量比例和孔隙率，尤其针对不同结构行播冠层四分量比例和孔隙率的变化规律进行分析。

2 POV-ray 的参数分析和验证

首先介绍 POV-ray，并对其系统参数进行敏感性分析；在此基础上，选择适当的参数设置，针对相同冠层分别用基于光线逆向追踪的 POV-ray 和基于辐射度的 RGM 模型(Radiosity-Graphics combined Model)(Qin & Gerstl, 2000)计算四分量比例，通过分析结果，验证 POV-ray 在应用于冠层四分量比例计算中的可靠性。所用冠层分为行播冠层和连续冠层，叶片为三角形，在冠层内为喜直型随机分布，具体冠层结构参数见表 1。

2.1 POV-ray 简介

POV-ray 是应用光线逆向追踪(即蒙托卡罗方法, Govaerts & Verstraete. 1998)绘制三维图像的开源软件(POV-team，2004)，其输出图像直观地表现了光线与实体(如植被叶片等)相互作用后的结果。作为一个计算高效、简洁易用的软件，POV-ray 广泛应用于生物化学、电路模拟、建筑设计和三维景观生成等领域。由于其开源的特点，可以保证各模块不断优化、完善，始终达到最优的效果。在对地遥感领域，近年有学者尝试引入：Sinoquet 等(1998)利用 POV-ray 模拟了冠层的三维光环境; Casa 和 Jones(2005)利用 POV-ray 进行了从多角度图像中反演叶面积指数的研究。

2.2 POV-ray 参数的敏感性分析

POV-ray 的输出是图像，根据四分量比例的定义，统计不同组分像元数与整幅图像像元总数之比，可得到视场中植被冠层四分量比例结果。通过对遥感成像过程的分析, POV-ray 中有 3 个参数可以对最后的结果产生较大影响，分别是：视场角(Field of View , FOV)，相机距地面距离和图像分辨率。对这 3 个参数分别进行敏感性分析，场景为表 1 中的行播冠层，此时垄行方向为南北方向，三角形叶片个数为 76800 个，太阳方位角(Sun Azimuth Angle, SAA)为 140° (向北的方向定义为 0°方位角，方位角顺时针增加，则东，南和西的方位角分别是 90°，180°和 270°)，太阳天顶角(Sun Zenith Angle, SZA)为 40°。文中取主平面(观测方位角(View Azimuth Angle, VAA)为 140°)进行分析，观测天顶角(View Zenith Angle, VZA)从前向 60°变化到后向 60°，每隔 5°成像一次。图 1 为 POV-ray 所得冠层四分量比例结果示例图，此时 VAA =140°, VZA=–45°,图像中绿色为亮叶，黑色为暗叶，白色为亮土，灰色为暗土。由于视场中，亮的组分对于辐射传输的贡献更大，后面的分析中只给出亮叶、亮土分量比例和孔隙率的演算结果。

表 1 用于 **POV-ray** 系统参数敏感性分析及结果验证的冠层结构统计参数

	LAI	株高/cm	行距/cm	行宽/cm	平均叶倾角/(°)	叶片最大面积/ cm^2	叶片最小面积/ cm^2	叶片平均大小/ cm^2
行播	1.28	30	50	20	61.89	12.5	0.2	10.7
连续	4.89	100	-	-	63.57	12.5	0.3	10.9

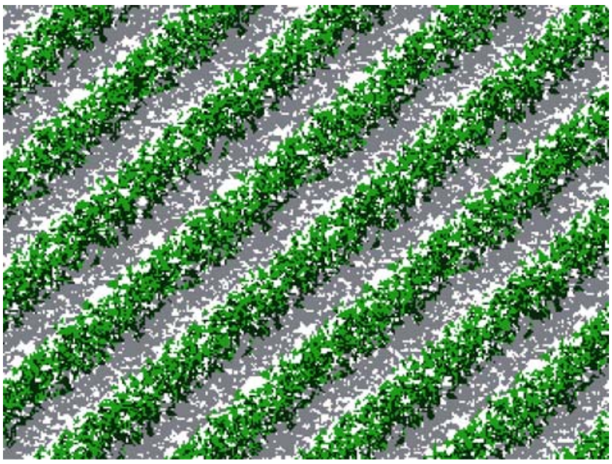

图 1 POV-ray 所得冠层四分量比例结果示例图

2.2.1 FOV 的影响

传感器视场面积由视场角和相机距地面距离共同决定，计算公式为:

$$S = (2 \times H \times \tan(FOV/2))^2 \tag{1}$$

式中, S 为视场面积, FOV 为视场角, H 为相机距地面距离。本文选取 FOV 分别为 0.01°，0.5°，10°，20°和 30°进行敏感性分析。为确保在不同的观测角度下，视场不超出场景，取地面面积 S=9.329m^2，在 FOV 变化的同时, H 也相应变化，以确保 S 不变,对应的相机

距离分别为 17500, 350, 17.46, 8.66 和 5.7m。输出图像的分辨率为系统默认的 320×240，此时图像像元大小为 1.215cm^2。图 2 为主平面(VAA=140°)分量结果图，可以得到亮叶、亮土分量在其他天顶角下没有太大的差异，但是在热点(VZA=40°)附近差异较大，视场角越小，热点效应越明显；孔隙率在天顶附近有差异，视场角越大孔隙率越小，均与理论相符。由于视场角为 0.5°和 0.01°时所得四分量比例在热点和天顶附近差异很小，而当视场角较小时，计算时间较长，因此在下文中统一设置视场角为 0.5°进行计算。

2.2.2 相机距离的影响

由式(1)可知在相同 FOV 下，相机距地面的距离(H)决定视场大小(S)，进而决定视场中的叶片总数，对四分量比例的结果有较大影响。因此，本文取 H 分别为 50, 200, 350 和 500m 进行敏感性分析，FOV 设置为 0.5°，其对应的 S 分别为 0.19，3.046，9.329 和 19.039m^2，输出图像的分辨率仍为 320×240，此时像元大小分别为 0.025，0.397，1.215 和 2.479 cm^2。图 3 为不同相机距离时主平面(VAA=140°)分量结果图，此时场景中单位垄行面积为 0.25m^2。当距离为 50m 时，对应的 S 为 0.19 m^2，视场中不能包含整垄冠层，因此结果波动较大；当视场面积大于 0.25m^2 后结果趋于一致，表明当视场面积大于完整的垄行单元后，四分量比例结果即可稳定，不再变化。考虑到运算效率和对结果的直观分析，在后面的运算中，在保证视场中包含完整垄行单元的前提下尽量取较小的相机距离。

2.2.3 图像分辨率的影响

图像分辨率是图像分辨能力的度量。本文选择 4 种分辨率进行敏感性分析，分别是 160×120，320×240, 640×480 和 1280×1024。FOV 设置为 0.5°，地面面积 S=9.329m^2，对应的像元大小为 4.859，1.215，0.304 和 0.071cm^2，输出 25 个结果所需的时间分别为：247，289，340 和 575s。图 4 为主平面(VAA=140°)分量结果图，可以看出在 4 个分辨率下结果差异不大，因为此时场景中叶片的平均大小为 10.7cm^2，均大于像元大小。考虑到运算时间和图像的直观分析等因素，在后面的运算中，尽量设置较低的分辨率进行计算。

2.3 POV-ray 与 RGM 结果一致性分析

RGM 模型是 Qin 和 Gerstl(2000)在 Goel 等(1991)的辐射度模型基础上改进发展起来的，经过参与一

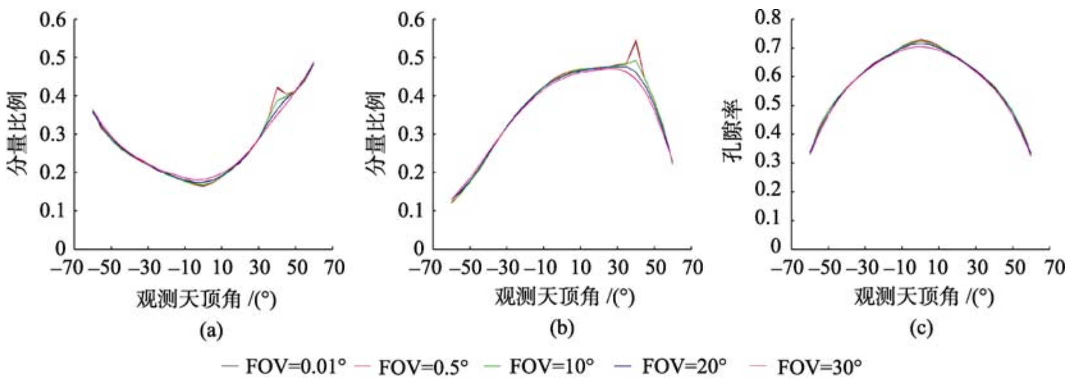

图 2 不同 FOV 时主平面分量结果图

(a) 亮叶分量; (b) 亮土分量; (c) 孔隙率

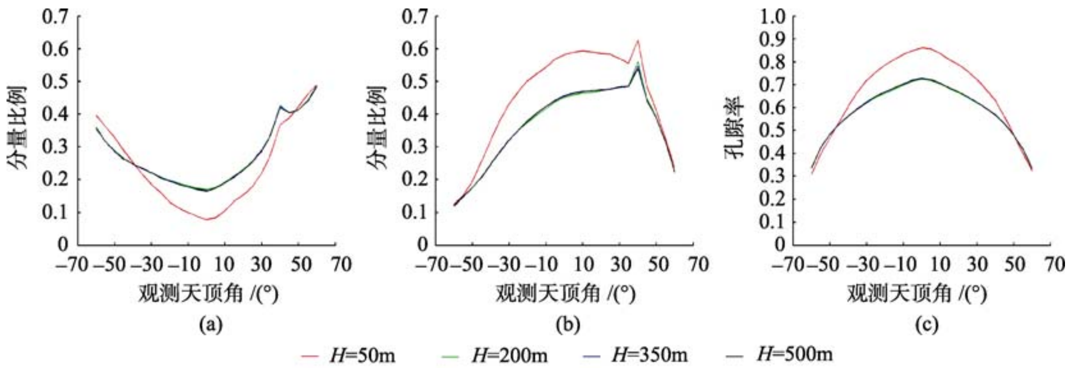

图 3 不同相机距地面距离时主平面分量结果图

(a) 亮叶分量; (b) 亮土分量; (c) 孔隙率

系列辐射传输模型的比较实验，其计算结果的可靠性得到认可(Pinty 等, 2004, Widlowski 等, 2007)。已有许多学者，如 Wu 等(2002)、Xie 等(2003)、Huang 等(2006)、Song 等(2007)和 Liu 等(2007)对其进行了改进和扩展。

POV-ray 是利用计算机图形学进行场景渲染成像的通用软件，在给定太阳和相机的几何关系、读入三维场景的位置坐标后，使用其自带的脚本语言进行编程即可计算视场的四分量比例和孔隙率。RGM 是基于辐射度原理计算多边形面元间的辐射传输过程，因此，它除了输入太阳、相机几何关系和三维场景位置坐标外，还要输入光谱信息，如光源特性、场景组分的反射率和透过率等，经过求解、计算可得场景的双向反射率因子和反照率等结果(Qin 和 Gerstl, 2000)。四分量比例只是 RGM 模型计算过程中产生的中间结果，但作为表征冠层几何结构的重要参数，四分量比例结果不随 RGM 输入的光谱信息的变化而改变。本文为验证 POV-ray 计算的四分量比例结果的可靠性，在太阳、相机几何关系和三维场景等输入条件一致的前提下，将 RGM 的四分量比例结果作为参考值，进行两者结果的比对。

将表 1 中冠层结构统计参数对应的两种场景分别用 POV-ray 和 RGM 计算不同角度下视场的四分量比例，方位角从 0°开始，每隔 10°为一个平面，各平面内由 0°—70°每隔 5°成像一次，共得 522 个结果，行播冠层垄向为南北方向。图 5 为 RGM 和 POV-ray 得到的连续冠层和行播冠层分量极化图。表 2 为两个模型所得的 522 个太阳—目标—相机观测几何下四分量比例的相关系数和 RMSE，可以得到两个模型结果具有很好的一致性。

通过对 POV-ray 的系统参数：FOV、相机距地面距离和图像分辨率进行敏感性分析；选择适当的

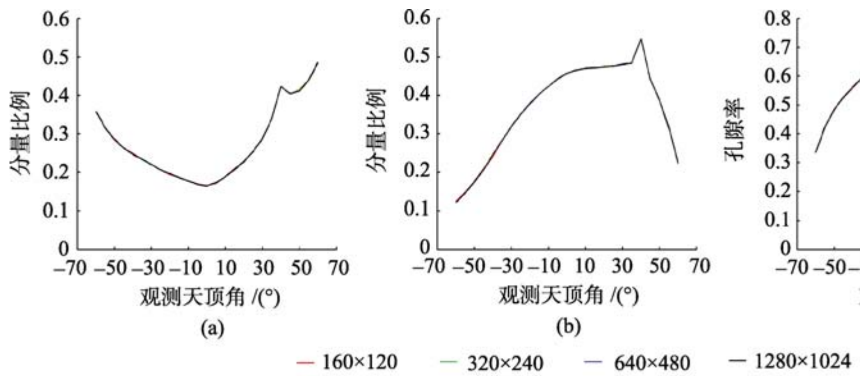

图 4 不同分辨率时主平面分量结果图

(a) 亮叶分量; (b) 亮土分量; (c) 孔隙率

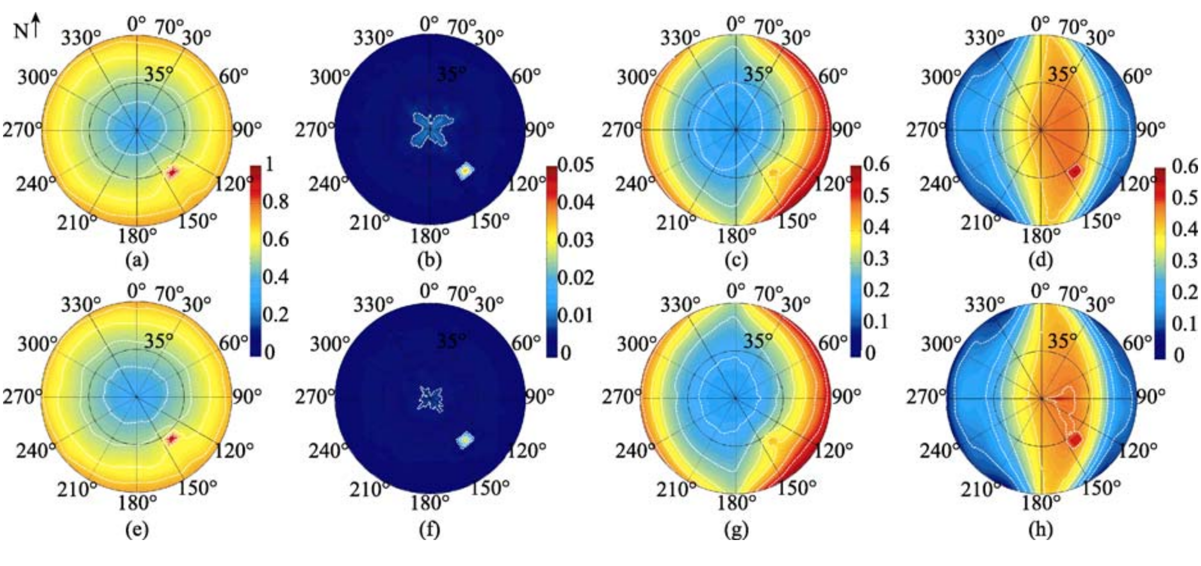

图 5 RGM 和 POV-ray 得到的分量极化图

(a) RGM 连续冠层亮叶分量; (b) RGM 连续冠层亮土分量; (c) RGM 行播冠层亮叶分量; (d)RGM 行播冠层亮土分量; (e) POV-ray 连续冠层亮叶分量; (f) POV-ray 连续冠层亮土分量; (g) POV-ray 行播冠层亮叶分量; (h)POV-ray 行播冠层亮土分量

表 2 统计结果

行播	亮叶	暗叶	亮土	暗土	连续	亮叶	暗叶	亮土	暗土
R^2	0.9993	0.9990	0.9988	0.9995	R^2	0.9976	0.9930	0.9491	0.9991
RMSE	0.0038	0.0030	0.0079	0.0082	RMSE	0.0137	0.0125	0.0016	0.0033

参数设置，计算植被冠层四分量比例；将结果与RGM 针对相同场景所得的四分量比例结果进行比对，得到 POV-ray 在应用于冠层四分量比例计算中的可靠性。

3 CLAMP 模型参数对四分量比例和孔隙率的敏感性分析

3.1 CLAMP 模型

CLAMP 模型能够模拟植被冠层的真实结构，该模型的特点是输入参数少，且与农学、遥感应用等直接相关，参数包括：种植模式*R*，植株密度*d*，集聚指数 *X*，叶片相对大小 *S* (热点参数)(Kuusk, 1985)，平均叶倾角(Average Leaf Angle，ALA) (Campbell, 1990)，叶片形状参数*B* (等腰三角形叶片底边与对应高的比)和叶面积指数(Leaf Area Index，LAI)。CLAMP 模型能普适、通用地模拟各种植被冠层，可根据具体的植被特征调整参数，具有较大的灵活性(Nadia 等, 2002)。

3.2 参数敏感性分析

本节针对 CLAMP 模型的主要参数对冠层四分量比例和孔隙率的影响进行敏感性分析。场景中叶片大小为 0.115cm^2，POV-ray 系统参数：FOV=0.5°，相机距离 *H*=60m，视场面积 *S*=0.273m^2，图像分辨率为 320×240，对应像元为 0.036cm^2。太阳位置固定在方位角 140°、天顶角 40°处。

3.2.1 种植模式和集聚指数变化分析

行播冠层与连续冠层的辐射特性存在很大差异(Jackson 等, 1979; Zhao 等, 2009)。CLAMP 模型中的种植模式控制植株的空间分布情况：*R*＝1 时表示叶片在以行宽、行距和行高限定的周期性平行垄行内分布；*R*＝0 时表示叶片在整个场景中连续分布。集聚指数控制冠层中叶与植株之间的水平距离：*X*=0 时表示叶株距离为 0，叶片完全呈集聚分布；*X*=1 时表示叶片完全随机分布，无集聚效应；当 *X* 的值介于 0—1 时，叶片的集聚程度也相应变化。

本文取 4 种情况进行敏感性分析，分别是：R_0X_0，代表连续冠层、叶片完全集聚分布；R_0X_1，代表连续冠层、叶片随机分布；R_1X_0，代表行播冠层、叶片完全集聚分布；R_1X_1，代表行播冠层、叶片随机分布；垄行走向为南北方向。CLAMP 模型的具体输入参数见表 3。

图 6 是种植模式和集聚指数变化时亮叶、亮土分量极化图，由图 6 可知：热点效应均较明显，在热点(VAA=140°，VZA=40°)附近，亮叶和亮土分量达到最大值；亮叶分量在叶片随机分布(*X*=1)的两种情况大于与之对应的叶片完全集聚(*X*=0)的两种情况，这是由于叶片完全集聚时，在视场中叶片间相互遮挡的概率比叶片随机分布的情况大，使得视场中任意观测角度下叶片的组分均小于随机分布的情况。当冠层为行播冠层(*R*=1)时，垄行结构均较明显，有一近似平行垄行方向的极值条带(亮叶为小值条带，亮土为大值条带)，行效应明显，特别是当叶片随机分布时，此时“碗边”效应也很明显；而当叶片完全集聚时，由于前述原因，在垂直垄行方向，当天顶角较小时出现类似垄行的条带。当冠层为随机连续冠层(*R*=0)、叶片随机分布时，无论亮叶分量还是亮土分量较为均一，只是在热点附近有一极大区域；当叶片完全集聚分布时，株与株之间的距离较大，导致极化图在圆心处呈发散状。

图 7 为种植模式和集聚指数变化时主平面(VAA=140°)分量结果图。当叶片随机分布(*X*=1)时，亮叶分量均大于叶片完全集聚(*X*=0)的情况，天顶和热点附近处尤为明显；完全集聚的情况比叶片随机分布的情况各向异性更明显，是因为此时叶片相互遮蔽概率较大，亮叶组分对观测天顶角的变化更为敏感；在相同集聚指数下，当观测天顶角较小时，连续冠层(*R*=0)的亮叶分量均大于对应的行播冠层(*R*=1)的，而当天顶角逐渐增大超过 20°左右后，行播冠层的亮叶分量反过来大于连续冠层的，其原因是行播冠层垄行内叶片密度大于连续冠层，大角度

表 3 种植模式和集聚指数变化时 CLAMP 参数设置

R	*X*	ALA/(°)	LAI	*S*	*B*	*d*/(株/m^2)	行距/cm	行宽/cm	株高/cm
0; 0; 1; 1	0; 1; 0; 1	58	2	0.2	0.3	400	10	5	20

观测时密集的叶片中更多的被照射和观测到；当叶片完全集聚分布时孔隙率各向异性最明显，当叶片随机分布时，行播冠层的孔隙率各向异性比连续冠层明显。

3.2.2 叶倾角变化分析

叶倾角分布函数(Leaf Angle Distribution, LAD)是描述植被冠层空间分布的重要参数，是叶片方位角和倾角的函数，通常情况下可假设叶片方位角对称分布。CLAMP 模型采用的是由 ALA 控制的单参数椭球分布函数控制叶片的倾角分布(Campbell, 1990)。Wang 等(2007)对几种常用的叶倾角分布函数进行比较，结果表明虽然椭球分布函数是单参数控制函数，但也较好的描述了冠层的叶倾角分布情况。本文取 3 种叶片倾角分布类型进行敏感性分析，分别是喜平型(ALA=10°)、近似球型(ALA=58°)和喜直型(ALA=75°), CLAMP 模型的具体输入参数见表 4。

图 8 是平均叶倾角变化时亮叶、亮土分量极化图，可以看到：亮叶分量随着叶倾角的增大，“碗边”效应逐渐增强，各向异性愈加明显；各分量的行效应也随着叶倾角的增大更加明显。

图 9 是叶倾角变化时主平面分量结果图。由图可知，主平面内热点效应明显，亮叶、亮土分量在热点处(VZA=40°)均达到最大值；当观测天顶角较小时，叶片喜平型分布的亮叶分量较喜直型分布得大，当观测天顶角逐渐增大时，喜直型分布的亮叶分量反过来大于喜平型分布的情况。喜平型分布的孔隙率，在观测天顶角较小时变化率较大，在较大天顶

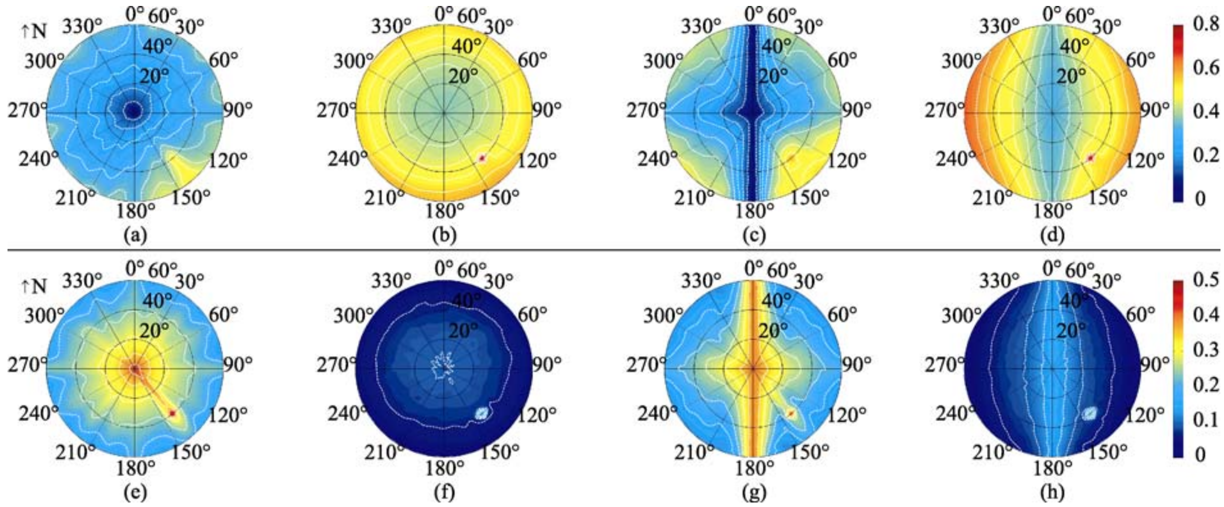

图 6 种植模式和集聚指数变化时分量极化图

(a) R_0X_0 时亮叶分量; (b) R_0X_1 时亮叶分量; (c) R_1X_0 时亮叶分量; (d) R_1X_1 时亮叶分量; (e) R_0X_0 时亮土分量; (f) R_0X_1 时亮土分量; (g) R_1X_0 时亮土分量; (h) R_1X_1 时亮土分量

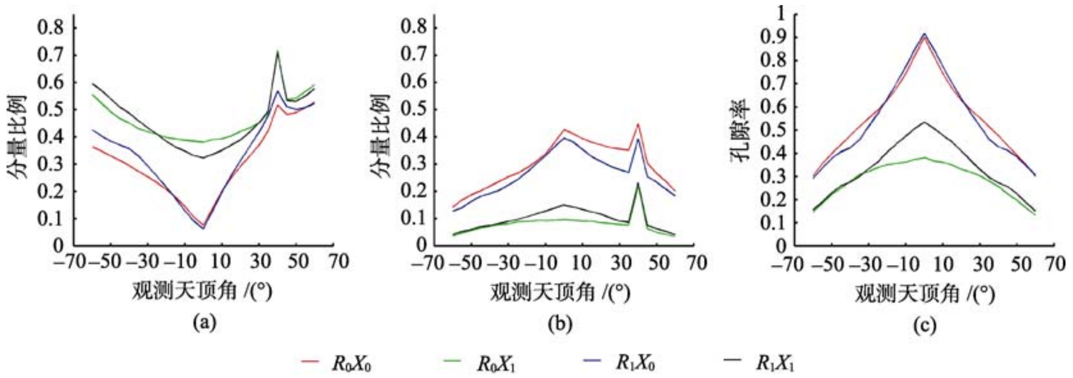

图 7 种植模式和集聚指数变化时主平面分量结果图

(a) 亮叶分量; (e) 亮土分量; (c) 孔隙率

表 4 ALA 变化时 CLAMP 参数设置

ALA/(°)	LAI	R	S	X	B	d/(株/m²)	行距/cm	行宽/cm	株高/cm
10; 58; 75	2	1	0.2	1	0.3	400	10	5	20

角观测时，孔隙率变化很小；喜直型分布的孔隙率对观测天顶角的变化一直较敏感。

3.2.3 叶面积指数变化分析

叶面积指数是单位地表面积上总叶面面积的一半，它控制着植被的许多生理、物理过程，如光合、呼吸和蒸腾等，是空间尺度上重要的冠层结构参数(Jonckheere 等, 2004)。

本文按照典型行播作物生长发展过程，选取 3 个阶段进行敏感性分析，分为作物生长早期、中期和晚期，LAI 分别为：1, 2 和 4，均为垄行结构，在行距保持不变的前提下，随着 LAI 的增大，相应的行宽、集聚指数也在变化，CLAMP 模型的具体输入参数见表 5。

图 10 是叶面积指数变化时亮叶、亮土分量极化图，图中直观的反映了行播作物生长期的变化规律，即亮叶分量逐渐增大，亮土分量逐渐减小；当 LAI=1 时，亮叶分量的热点效应和垄行效应都不明显，是因为此时叶面积指数较小，场景中叶片所占

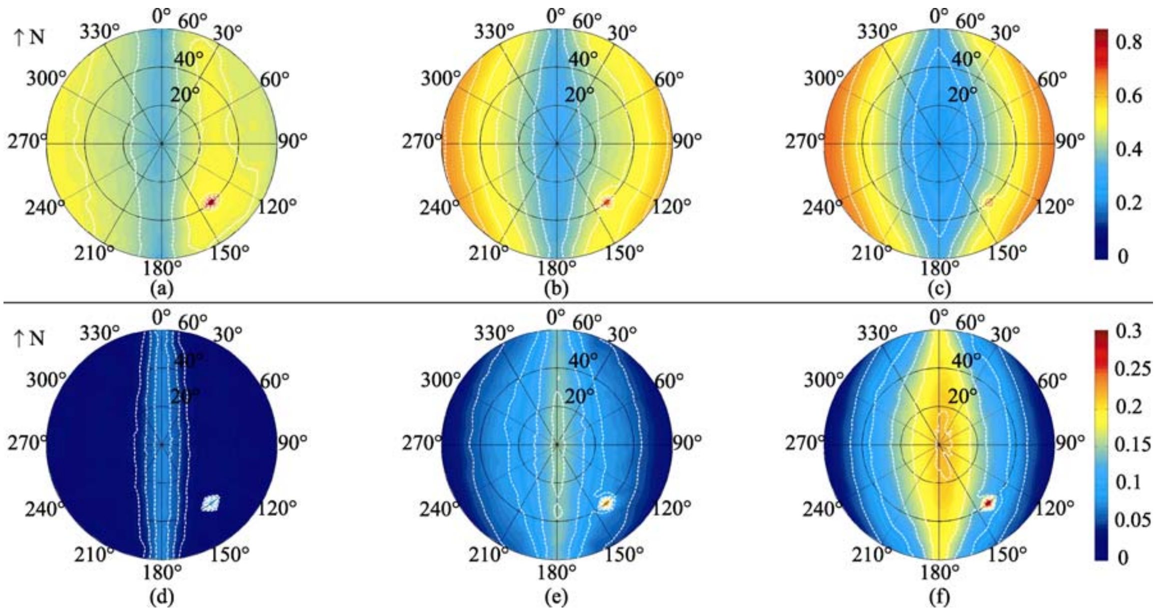

图 8 平均叶倾角为 10°, 58°, 75°时分量极化图

(a) 10°时亮叶分量; (b) 58°时亮叶分量; (c) 75°时亮叶分量; (d) 10°时亮土分量; (e) 58°时亮土分量; (f) 75°时亮土分量

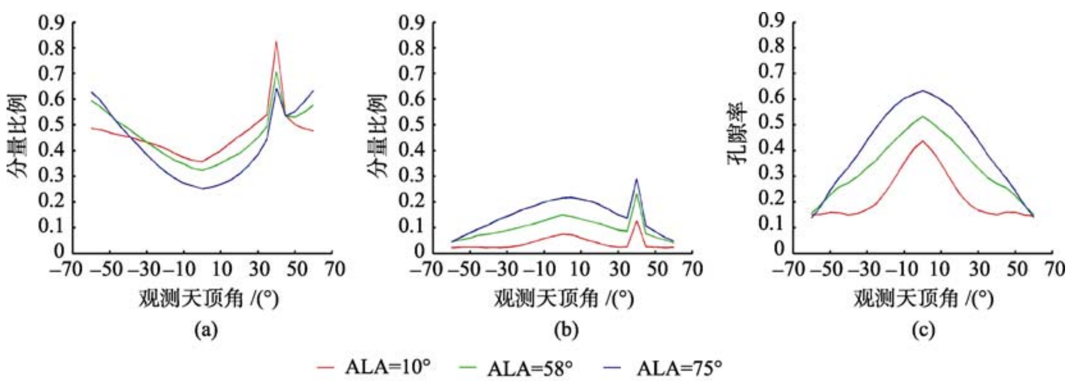

图 9 叶倾角分布变化时主平面分量结果图

(a) 亮叶分量; (b) 亮土分量; (c) 孔隙率

表 5 LAI 变化时 CLAMP 参数设置

	LAI	X	行宽/cm	ALA/(°)	R	S	B	d/(株/ m^2)	行距/cm	株高/cm
初期	1	0.3	3	58	1	0.2	0.3	400	10	20
中期	2	0.5	5	58	1	0.2	0.3	400	10	20
后期	4	0.8	9	58	1	0.2	0.3	400	10	20

的比例不大，且较集聚于植株分布(X=0.3)，植株比较稀疏，视场中更多的土壤被照射和观测到；当LAI=2 时，热点效应、“碗边”效应和垄行结构均较明显，此时场景中叶片增多，且集聚指数 X=0.5，行宽=5cm，是典型的行结构冠层。在垂直垄行方向有一类似垄行的条带，是由于叶片受集聚指数控制，在垄行内并不是完全连续分布，植株间存在较大空隙；当 LAI=4 时，热点、“碗边”效应明显，垄行结构并不明显，其原因是此时叶片较多，集聚指数 X=0.8，行宽=0.9cm，叶片在冠层内十分接近于连续分布，虽然亮土在垄行方向有一大值区域，但是其值很小。

图 11 为叶面积指数变化时主平面分量结果图。可以看到，当 LAI=1 时亮叶分量的热点效应十分微弱，其值相比其他两种情况小很多，而亮土分量的热点效应较明显，其值也比其他两种情况大很多；此时孔隙率最大，各向异性不明显。当 LAI=2 时，热点效应、“碗边”效应均较明显，孔隙率较大，各项异性最明显。当 LAI=4 时，场景中叶片比例是 3 种情况中最大的，热点效应和“碗边”效应均较明显，孔隙率较小，且各向异性较明显。

4 结 论

POV-ray 采用光线逆向追踪方法进行三维场景成像，以其强大的计算能力和方便、简洁的命令语言，已在三维场景仿真和可视化等领域得到广泛应用，但在遥感中的应用较少。本研究利用 POV-ray 快速

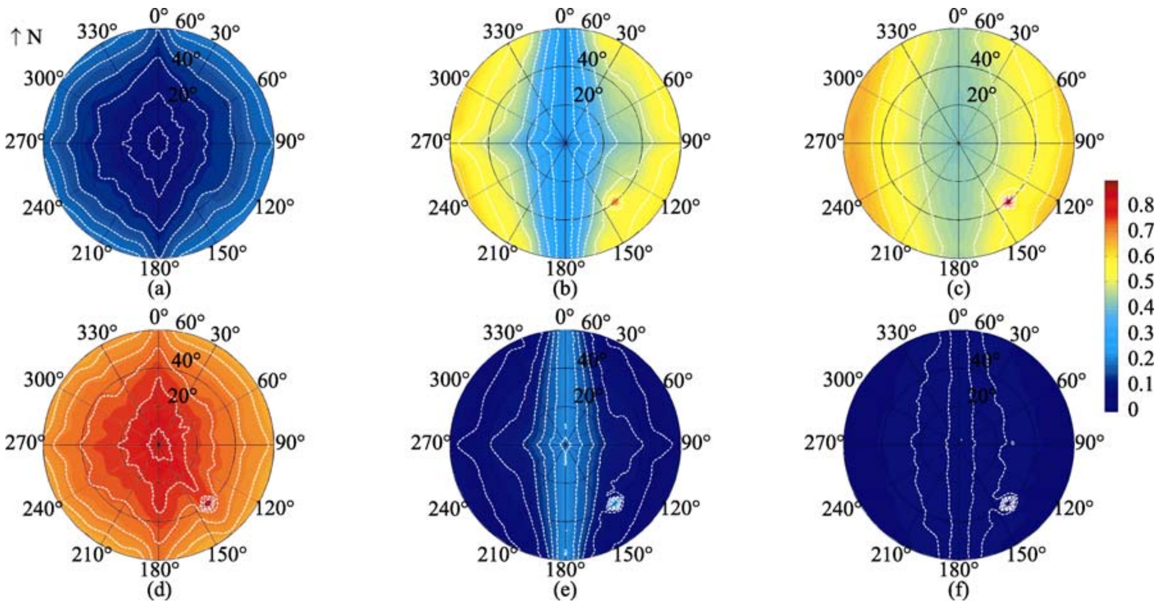

图 10 LAI=1,2,4 时分量极化图

(a) LAI=1 时亮叶分量; (b) LAI=2 时亮叶分量; (c) LAI=4 时亮叶分量; (d) LAI=1 时亮土分量; (e) LAI=2 时亮土分量; (f) LAI=4 时亮土分量

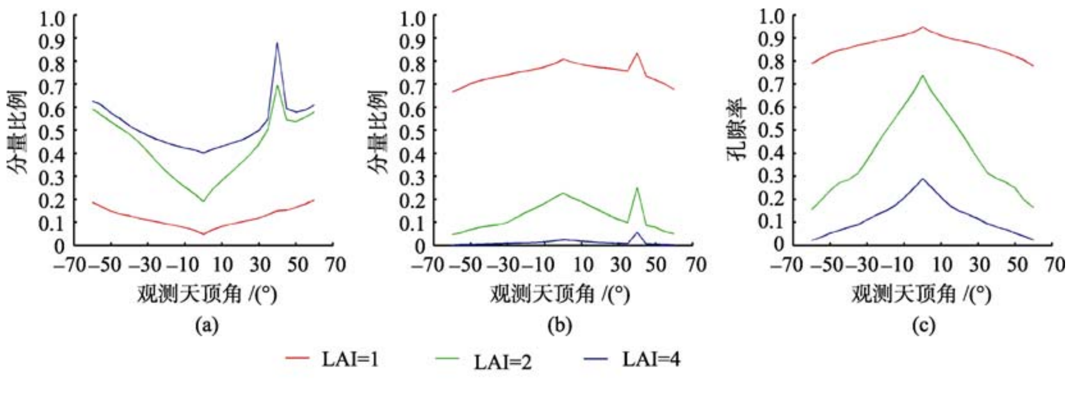

图 11 叶面积指数变化时主平面分量结果图

(a) 亮叶分量; (b) 亮土分量; (c) 孔隙率

计算植被真实结构模型 CLAMP 生成的复杂冠层的四分量比例和孔隙率，其计算效率较高，结果直观的显示了不同观测角度下冠层四分量比例和孔隙率的变化情况，是进行定量遥感研究有利的工具。

本文以典型农作物的四分量比例和孔隙率为考察对象，对 CLAMP 模型的主要输入参数进行敏感性分析，结果表明：当冠层垄行结构明显时，相对于其他因素，行效应对于四分量比例和孔隙率的影响占主导，因此，当植被冠层为垄行结构时，其四分量比例和孔隙率的变化较连续冠层更加复杂；集聚指数可以有效的控制叶片的空间分布模式，进而影响视场中植被与土壤的相对面积比例，对于四分量比例和孔隙率结果有较大影响；叶倾角分布类型对四分量比例和孔隙率结果的各向异性特征影响明显，当平均叶倾角越大时，所得结果各向异性越明显；本文还比较了垄行作物的 3 个典型生长期的四分量比例变化情况，在作物生长初期土壤对结果影响更大，到作物生长后期植被对结果的影响占主导，亮叶分量各向异性特征较为明显。

本研究初步表明 POV-ray 可准确、快速的计算植被遥感中的重要参数：四分量比例和孔隙率，并能有效的用于植被主要结构参数的敏感性分析，在遥感机理研究中有较大的应用潜力。在以后的工作中，可进一步研究 POV-ray 在三维场景真实再现及不同光照入射情况下的光影渲染技术，计算定量遥感研究更感兴趣的方向反射率因子和反照率等参数。

致 谢 Casa 教授和 POV-ray team 在使用 POV-ray 时提供了有益的指导和帮助；北京林业大学的黄华国博士和北京师范大学的陈敏、谢东辉博士和宋金玲博士在使用 RGM 模型进行模型比较验证时给予了大量帮助，在此一并表示感谢。

REFERENCES

Bruno A, Yassine S and Nicolas I. 1994. A direct method to measure bidirectional gap fraction in vegetation canopies, *Remote Sensing of Environment*, **50**(1): 61—66

Casa R and Jones H G. 2005. LAI retrieval from multiangular image classification and inversion of a ray tracing model. *Remote Sensing of Environment*, **98**(4): 414—428

Campbell G S. 1990. Derivations of an angle density function for canopies with ellipsoidal leaf angle distributions. *Agricultural and Forest Meteorology*, **49**(3): 173—176

Gower S T, Kucharik C J and Norman J M.1999. Direct and indirect estimation of leaf area index, fAPAR, and net primary production of terrestrial ecosystems. *Remote Sensing of Environment*, **70**(1): 29—51

Goel N S, Rozehnal I and Thompson R L. 1991. A computer graphics based model for scattering from objects of arbitrary shapes in the optical region. *Remote Sensing of Environment*, **36**(2): 73—104

Govaerts Y M and Verstraete M M. 1998. Raytran a monte carlo ray-tracing model to compute light scattering in three-dimensional heterogeneous media. *IEEE Transactions on Geoscience and Remote Sensing*, **36**(2): 493—505

Huang H G, Qin W H, Liu Q H, Liu Q and Li X W. 2006. An extended radiosity-graphics model for directional brightness temperature research. *IGARSS*

Jackson R D, Reginato R J, Pinter P J and Idso S B. 1979. Plant canopy information extraction from composite scene reflectance of row crops. *Applied Optics*, **22**(18) :3775—3782

Jonckheere I, Fleck S, Nackaerts K, Muys B, Coppin P, Weiss M and Baret F. 2004. Review of methods for in situ leaf area index determination Part I. Theories, sensors and hemispherical photography. *Agricultural and Forest Meteorology*, **121**(1—2): 19—35

Kimes D S. 1983. Remote sensing of row crop structure and component temperatures using directional radiometric temperatures and inversion technique. *Remote Sensing of Environment*, **13**: 33—55

Kimes D S, Norman J M and Walthall C L. 1985.Modeling the radiant transfers of sparse vegetation canopies. *IEEE Transactions on Geoscience and Remote Sensing*, **23**(5): 659—704

Kuusk A. 1985. The hot spot effect of a uniform vegetative cover. *Soviet Journal Remote Sensing*, **3**(4): 645—658

Li X W and Strahler A H. 1985. Geometiric-optical modeling of a conifer forest canopy. *IEEE Transactions on Geoscience and Remote Sensing*, **23**(5): 705—721

Li X W and Strahler A H. 1986. Geometiric-optical reflectance modeling of a conifer forest canopy. *IEEE Transactions on Geoscience and Remote Sensing*, **24**(66): 906—919

Liu Q H, Huang H G, Qin W H, Fu K H and Li X W. 2007. An extended 3D radiosity-graphics combined model for studying thermal emission directionality of crop canopy. *IEEE Transactions on Geoscience and Remote Sensing*, **45**(9): 2900—2918

POV-team. 2004. Introduction to POV-Ray for POV-Ray Version 3.6.1. http://www.povray.org

Pinty B, Widlowski J L, Taberner M, Gobron N, Verstraete M M, Disney M, Gascon F, Gastellu J P, Jiang L, Kuusk A, Lewis P, Li X, Ni-Meister W, Nilson T, North P, Qin W, Su L, Tang S, Thompson R, Verhoef W, Wang H, Wang J, Yan G and Zang H. 2004. Radiation transfer model intercomparison

(RAMI) exercise: Results from the second phase . *Journal of Geophysical Research*, **109**, D06210, doi:10.1029/ 2003JD 004252

Qin W H and Gerstl S A W. 2000. 3-D scene modeling of semidesert vegetation cover and its radiation regime. *Remote Sensing of Environment*, **74**(1): 145—162

Rochdi N, Baret, F, Combal B and Chelle M. 2002. CLAMP: A model of leaf clumping in canopies. Recent Advances in Quantitative Remote Sensing, 1st International Symposium, Spain, Publications of the University of Valencia

Sinoquet H, Thanisawanyangkura S, Mabrouk H and Kasemsap P. 1998. Characterization of the light environment in canopies using 3D digitising and image processing. *Annals of Botany*, **82**(2): 203—212

Song J L, Wang J D and Liu X Q. 2007. Computer simulations of difering radiation regimes on aspen trees. *Journal of Remote Sensing*, **11**(5): 669—676

Widlowski J L, Taberner M, Pinty B and Bruniquel-Pinel V, Disney M, Fernandes R, Gastellu-Etchegorry J P, Gobron N, Kuusk A, Lavergne T, Leblanc S, Lewis P E, Martin E, Mottus M, North P R J, Qin W, Rpbustelli M, Rochdi N, Ruiloba R, Soler C, Thompson R,Verhoed W, Verstraete M M and Xie D. 2007. The third radiation transfer model intercomparison (RAMI) exercise: Documenting progress in canopy reflectance modeling. *Journal of Geophysical Research,* 112: doi 10.1029/ 2006JD007821

Wu M X, Zhu Q J, Su L H, Wang J D, Xiang Y Q, Tang S H and Wang P X. 2002. The 3-D scene computer simulation of the field crop canopy. Recent Advances in Quantitative Remote Sensing, 1st International Symposium, Spain, Publications of the University of Valencia

Wang W M, Li Z L and Su H B. 2007. Comparison of leaf angle distribution functions: Effects on extinction coefficient and fraction of sunlit foliage. *Agricultural and Forest Meteorology*, **143**(1—2): 106—122

Xie D H, Wu M X, Zhu Q J, Wang J D and Tang S H. 2003. Quantitative remote sensing research on the vegetation 3-D visual simulation based on object oriented technique. *IEEE International Geoscience and Remote Sensing Symposium*. **6**: 3922—3924

Zhao F, Gu X F, Wout Verhoef, Wang Q, Yu T, Liu Q, Huang H G, Qin W H, Chen L F and Zhao H J, 2010, A spectral directional reflectance model of row crops, *Remote Sensing of Environment*, **114**(2): 265—285